

# ZEUS-3D 2-D Gallery #4: The Hydrodynamical Kelvin-Helmholtz Instability

## Linear Regime

Two layers of fluid sliding past each other with *relative* speed  $2v_0$  form a *shear layer* (Fig. 1) which is subject to the *Kelvin-Helmholtz instability* (KHI) for certain ranges of the *relative* Mach number,  $2M$ , where  $M = v_0/c_s$  and  $c_s$  is the sound speed. To approach this problem *analytically*, one examines perturbations to the linearised fluid equations, from which the following conclusions may be drawn:

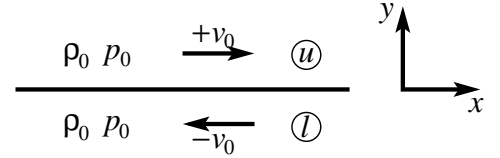


Figure 1: A shear layer.

1. Where the shear layer is unstable, the perturbation growth rate is  $\propto 1/\lambda$ , where  $\lambda$  is the wavelength;
2. The shear layer is most unstable for  $2M = 3^{1/2} \sim 1.73$ ;
3. For  $2M > 2^{3/2} \sim 2.83$ , the shear layer is unconditionally stable to perturbations.

The first conclusion cannot be true indefinitely since, at some point, the effects of viscosity and/or surface tension damp out the perturbations before they can grow.

To compare numerical results with the predictions from linear theory, twelve `dzeus36` simulations of a shear layer with  $\rho_0 = 1$ ,  $c_s = 1$ ,  $\vec{B} = 0$ , and  $0.25 \leq 2M \leq 3.0$  in increments of 0.25 were performed on a 2-D domain  $(x, y) = (-0.5:0.5, -0.5:0.5)$  on a  $500 \times 500$  uniform zone Cartesian grid. Two “buffer regions”,  $(x, y) = (-0.5:0.5, -10.0:-0.5)$  and  $(x, y) = (-0.5:0.5, 0.5:10.0)$ , each resolved by  $500$  (uniform)  $\times$   $150$  (ratioed) zones, were included to insulate the domain from unwanted reflections from the upper and lower boundaries<sup>1</sup>. Periodic boundary conditions were imposed on the left and right boundaries.

The shear layer is established by setting  $v_x = v_0 \tanh(y/y_s)$  where  $y_s = 0.02$  domain widths, for a total shear layer “thickness” of 0.04 resolved with 20 zones. The non-zero thickness of the shear layer is to prevent minute numerical perturbations from breaking up an under-resolved shear layer into small vortex tubes. Once established, the shear layer is perturbed with a sinusoidal transverse velocity of amplitude 0.001 and wavelengths ranging from 0.25 to 1. Simulations are carried on to  $t = 12$  and performed with

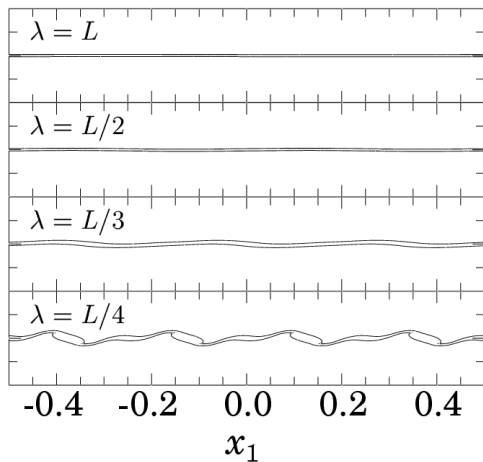


Figure 2: *ZEUS-3D* images showing the development of the KHI for  $2M = 1.5$  at  $t = 0.75$ , where  $t = 1$  is the time for a sound wave to travel a distance  $L = 1$  (the width of the grid). These results agree qualitatively with the first of the predictions from linear theory given above, namely that the growth rate is inversely proportional to the wavelength. Note that non-linear effects are already apparent in the  $\lambda = L/4$  case.

<sup>1</sup>Others have used reflecting boundary conditions at  $y = \pm 0.5$  with success (*e.g.*, [Ryu et al., 2000, ApJ, 545, 474](#)), but this works only for Mach numbers  $2M < 1.2$ . At higher speeds, shocks are excited and the region above and below the shear layer become dynamically important.

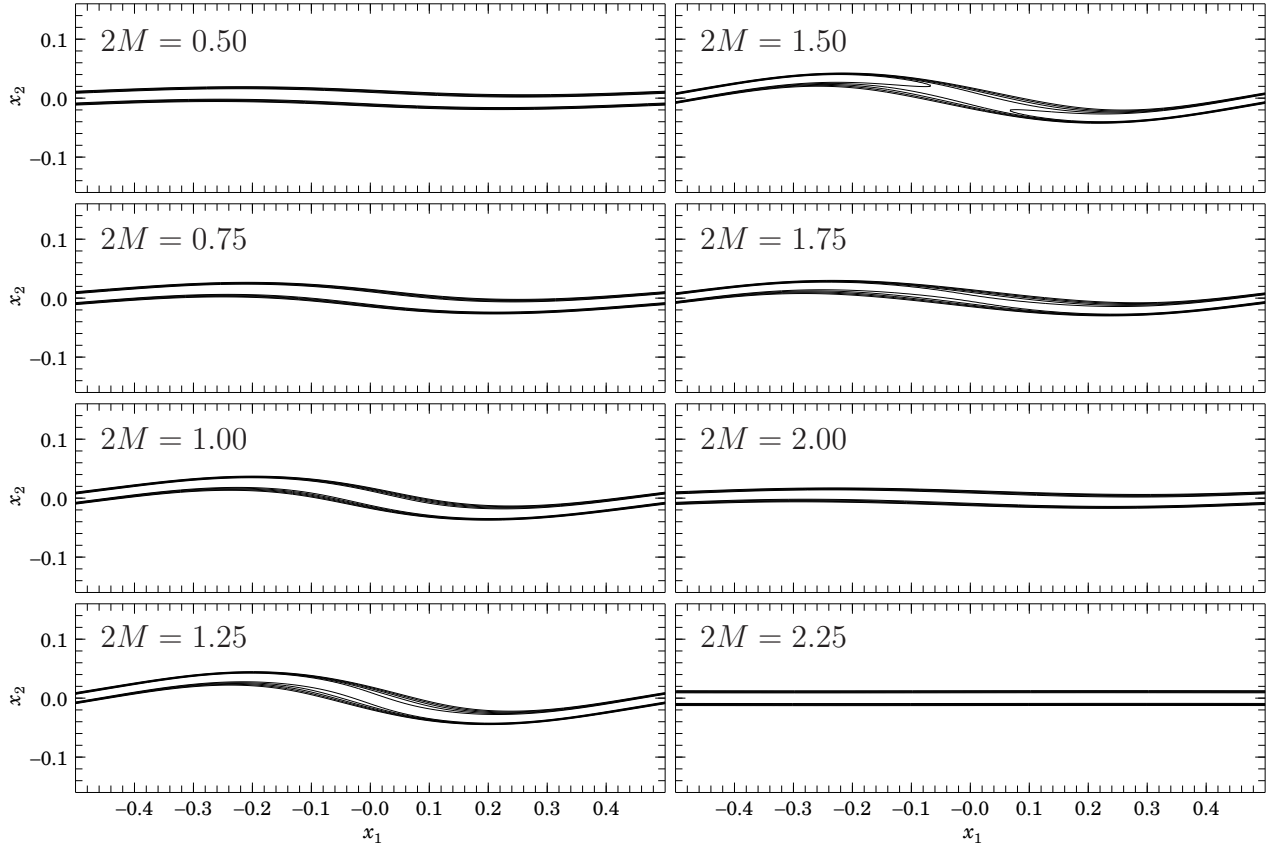


Figure 3: *ZEUS-3D* images showing the development of the KHI after  $t = 2.6$  for the relative Mach numbers indicated. Highest growth rate is for  $1.25 < 2M < 1.5$ , whereas linear theory predicts highest growth rate at  $2M = 1.73$  (second prediction above). This discrepancy may result from the non-zero thickness of the numerical shear layer, as opposed to the infinitesimally thin shear layer assumed by linear theory. Not shown are  $2M = 2.5$  and  $2.75$  which grow too slowly to be seen at  $t = 2.6$  (but develop by  $t = 12$ ), and  $2M = 3.0$  which remains stable through  $t = 12$ . Linear theory predicts stability at  $2M = 2.83$  (third prediction above).

CMoC, FIT (*Finely Interleaved Transport*; see the [2-D advection page](#)) using the internal energy equation, artificial viscosity `qcon=2` and `qlin=0.2`, and Courant number `courno=0.75` for  $0.25 \leq 2M \leq 1.75$  and `courno=0.5` for  $2.0 \leq 2M \leq 3.0$ . The lower Courant number at higher relative Mach numbers is to suppress a peculiar numerical “instability” discussed below.

Figures 2 and 3 above show contour images of the normal component of the vorticity ( $\omega_{\perp}$ ; effective at visualising the shear layer) for many of these simulations before the onset of non-linearity. Discussion and comparison of these results with the three predictions from linear theory are found in the figure captions.

## Non-linear Regime

Figure 4 shows colour contours of  $\omega_{\perp}$  at  $t = 12$  (well beyond the linear regime) for each of the twelve simulations with relative Mach numbers as indicated. Each image is hyper-linked to its animation.

For  $2M > 1$  (supersonic relative speeds), shocks are excited above and below the shear plane which engage much more of the external medium than when  $2M \leq 1$  (hence the “buffer zones”). As initialised (top half moving right, bottom left),  $\omega_{\perp} = \partial_x v_y - \partial_y v_x < 0$  in the shear layer (red through blue with deep blue being the most negative), and  $\omega_{\perp} = 0$  above and below the shear layer (salmon). Lighter shades of

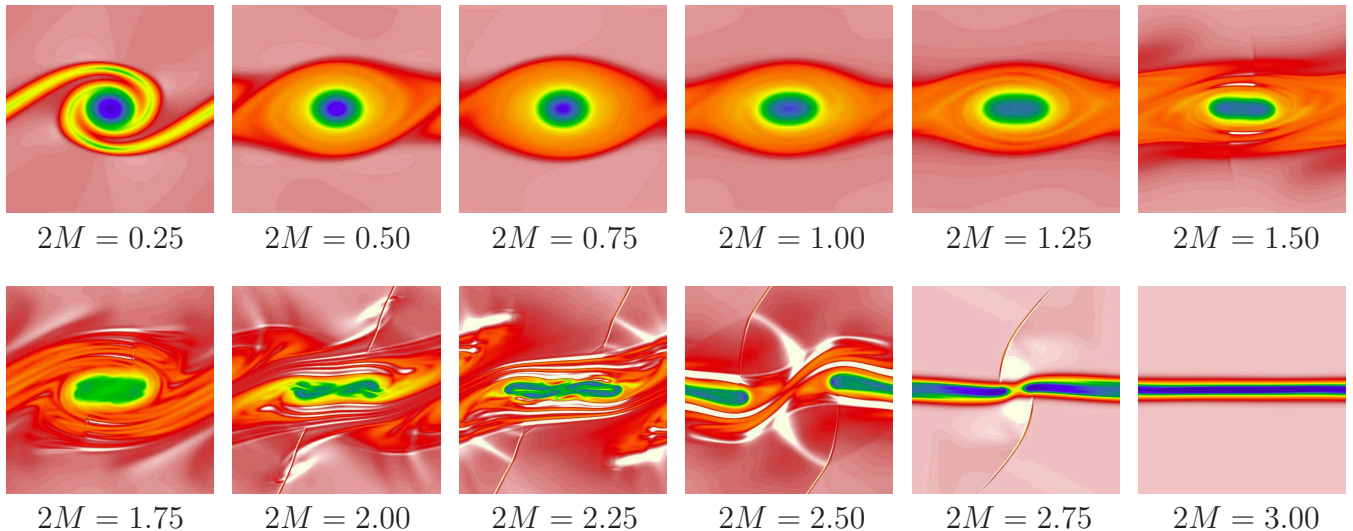


Figure 4: End-states of *ZEUS-3D* simulations showing colour contours of  $\omega_{\perp}$  (click on an image for its animation). Salmon through white indicate  $\omega_{\perp} > 0$ ; red through blue  $\omega_{\perp} < 0$ , with blue being the most negative.

salmon through white correspond to regions of positive  $\omega_{\perp}$ , possible only when strong shocks are excited.

The formation of a “cat’s eye” (a sustained vortex tube prominent near the end of most simulations) is a well-known effect which has been observed for decades in simulations performed by finite-difference codes<sup>2</sup>. It is the end state for all unstable Mach numbers, with the most rapid growth at  $2M \sim 1.5$ . However, by  $2M = 2.75$ , the growth rate of the perturbation has slowed sufficiently that the shear layer has only begun to trip into forming the vortex by  $t = 12$  and, at  $2M = 3$ , the original shear layer is still completely intact, in keeping with the third prediction above from linear theory.

## Periodic Boundary Conditions

Unlike an unsplit scheme where boundary conditions must be applied only at the end of each MHD cycle, boundary conditions must be applied frequently during each MHD cycle in *ZEUS-3D* owing to its operator and directionally/planar split methods. A significant effort has been made to ensure that boundary conditions are applied as often as needed (but only as often as needed) so that periodicity is maintained to machine accuracy. The same is true for all flavours of the reflecting boundary conditions.

Figure 5 shows the end results of a simulation for the  $2M = 1$  shear layer initialised identically to the one above except with two full periods of the perturbation, and thus a grid width of  $L = 2$ . Shown are  $\omega_{\perp}$  (top) and density (bottom), each hyper-linked to its animation. To within machine accuracy, each period is identical to the other in all variables, indicating the left- and right-boundary zones behave exactly as the central column of zones.

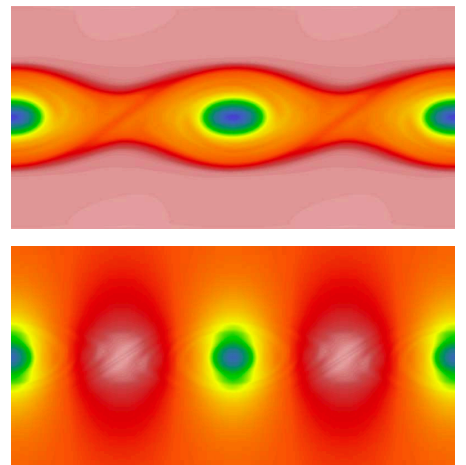


Figure 5: Two periods of the  $2M = 1$  shear layer,  $\omega_{\perp}$  top, density bottom.

<sup>2</sup>Historically, SPH codes have had great difficulty in simulating the KHI. However, relatively recent progress in SPH design has led to significant improvements (*e.g.*, Price, 2008, *J. Comput. Phys.*, 2008, 227, 10040).

# An Unexplained Numerical Instability

Figure 6 shows the  $2M = 2.25$  simulation at  $t = 7.5$  (just before the strong shocks above and below the shear layer are triggered) performed with four different transport algorithms and three different Courant numbers, to illustrate a peculiar (read: I don't understand it yet) numerical *shear “instability”* that I've seen only in these shear layer simulations. The “instability” is obvious in the `itote=1, courno=0.75` panels and, upon close examination of the `itote=0, courno=0.75` and `itote=1, courno=0.5` panels, one can see rather fine, nearly vertical striping in the salmon-coloured regions as well. These oscillations are rather well resolved (about ten zones per period regardless of the resolution of the simulation), form more rapidly at higher  $2M$ , saturate in amplitude (and thus why I have “instability” in quotations as most numerical instabilities grow without bound), and are stabilised once the strong shocks form. Thus, despite its dependence on the Courant number, I do not believe this to be a CFL violation. Note that in panels `itote=0, courno=0.5` and `itote=1, courno=0.25`, there is no sign of the shear instability whatever.

The first point to make is regardless of  $2M$  and for `courno` low enough to avoid the shear instability, it matters very little whether the non-conservative internal energy equation (`itote=0`) or the conservative total energy equation (`itote=1`) is solved. Examining the end-state of the animations for `itote=0, courno=0.5` and `itote=1, courno=0.25` shows only the slightest of quantitative differences between the two. A more detailed comparison (*e.g.*, of integrated conserved quantities over the course of the simulations) verifies this impression. That said, the total energy equation is clearly more susceptible to the shear instability than the internal energy equation, and thus the reason `itote=0` was used for Fig. 4.

Second point: both Legacy transport and FIT seem to be equally susceptible to the shear instability, and thus I conclude it is unrelated to the “striping instability” documented in the [2-D advection page](#) for which FIT provides a total cure. Indeed, what seems to “cure” the shear instability is a sufficiently low value of `courno`. Unlike the striping instability for which a lower Courant number merely *delays* its onset and *slows* its growth, a sufficiently low value for `courno` seems to completely rid the simulation of the shear instability, as illustrated in Fig. 6.

Third point: increasing either form of artificial viscosity can also “cure” the problem, but this is probably because, as a consequence, the time step is decreased. Thus, I don't believe this to be an upwindedness problem either, which artificial viscosity is supposed to stabilise.

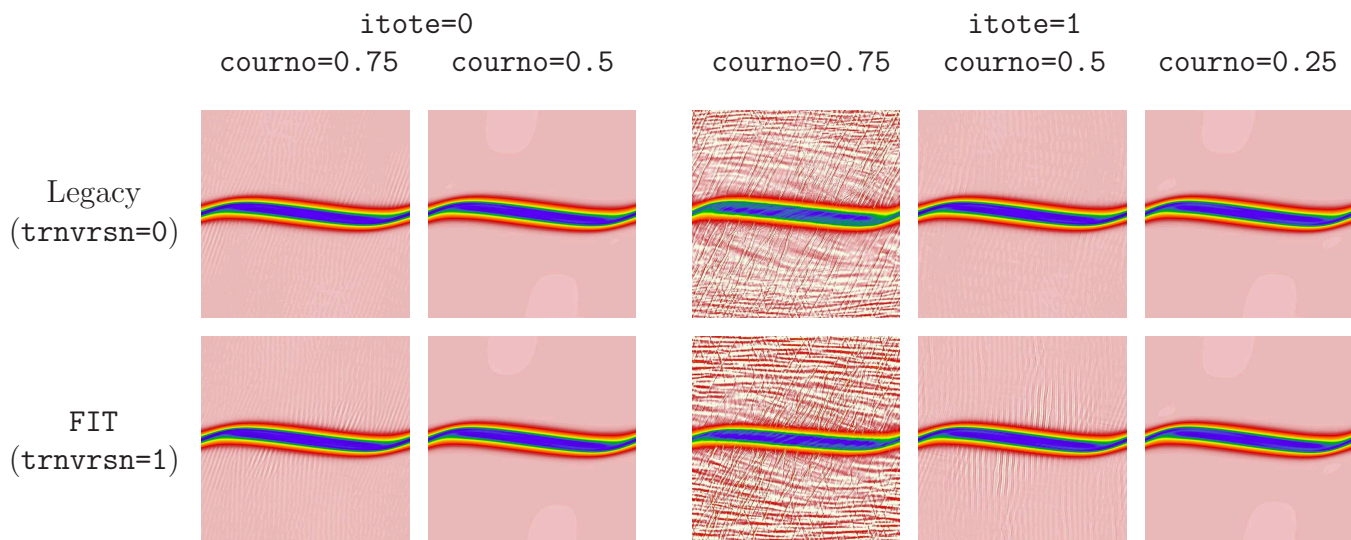


Figure 6: The normal vorticity of the  $2M = 2.25$  shear layer at  $t = 7.5$ , just before the onset of the shocks and the formation of the vortex, using various `dzeus36` algorithms and Courant numbers. Click any image for the corresponding animation which goes to  $t = 12$ .

It is clearly hydrodynamical in nature— $\vec{B} = 0$  in these simulations—and clearly agitated by the pending formation of the shocks. Other than that, I can offer little insight into the origin of this phenomenon and would be delighted to hear from anyone who may be able to help. In the meantime, users should consider themselves duly warned!

## Kelvin-Helmholtz Instabilities in Nature

The atmosphere surrounding a rapidly rotating planet is a particularly good natural laboratory for the KHI since the Coriolis effect is forever driving shear layers with relative speeds comparable to the rotation speed of the planet. On the Earth, low relative Mach number KHI are occasionally observed in high clouds (Fig. 7). By comparison and with its higher rotation speed, the Jovian atmosphere is replete with KHI including the Great Red Spot (observed since Galileo’s time), the most spectacular example of a sustained cat’s eye in the solar system (Fig. 8).



Figure 7: Clouds forming along shear layers separating air masses of differing moisture and temperature are subject to the K-H instability (photo credit: Brooks Martner, NOAA/ETL).



Figure 8: Jupiter’s Great Red Spot is a “cat’s eye” sustained by transonic shear layers in the planet’s atmosphere. Note the numerous other examples of KHI in the red spot’s vicinity. (photo credit: NASA).